Cancer Letters 419 (2018) 30–39

Contents lists available at ScienceDirect

Cancer Letters

journal homepage: www.elsevier.com/locate/canlet

Original Articles

The therapeutic potential of human adipose-derived mesenchymal stem cells producing CXCL10 in a mouse melanoma lung metastasis model

Hamed Mirzaei [a], Hossein Salehi [b], Reza Kazemi Oskuee [a], Ali Mohammadpour [c], Hamid Reza Mirzaei [d, e], Mohammad Reza Sharifi [f], Reza Salarinia [g], Hossein Yousofi Darani [h], Mojgan Mokhtari [i], Aria Masoudifar [j], Amirhossein Sahebkar [k, l, *], Rasoul Salehi [f, **], Mahmoud Reza Jaafari [m, n, ***]

[a] Department of Medical Biotechnology, School of Medicine, Mashhad University of Medical Sciences, Mashhad, Iran
[b] Department of Anatomical Sciences, School of Medicine, Isfahan University of Medical Sciences, Isfahan, Iran
[c] Faculty of Nursing and Midwifery, Gonabad University of Medical Sciences, Gonabad, Iran
[d] Department of Immunology, School of Medicine, Tehran University of Medical Sciences, Tehran, Iran
[e] Department of Clinical Laboratory Sciences, School of Allied Medical Sciences, Kashan University of Medical Sciences, Kashan, Iran
[f] Department of Genetics and Molecular Biology, School of Medicine, Isfahan University of Medical Science, Isfahan, Iran
[g] Department of Medical Biotechnology, School of Medicine, North Khorasan University of Medical Sciences, Bojnourd, Iran
[h] Department of Medical Parasitology and Mycology, School of Medicine, Isfahan University of Medical Sciences, Isfahan, Iran
[i] Department of Pathology, School of Medicine, Isfahan University of Medical Sciences, Isfahan, Iran
[j] Department of Molecular Biotechnology, Cell Science Research Center, Royan Institute for Biotechnology, ACECR, Isfahan, Iran
[k] Biotechnology Research Center, Pharmaceutical Technology Institute, Mashhad University of Medical Sciences, Mashhad, Iran
[l] Neurogenic Inflammation Research Center, Mashhad University of Medical Sciences, Mashhad, Iran
[m] Nanotechnology Research Center, Pharmaceutical Technology Institute, Mashhad University of Medical Sciences, Mashhad, Iran
[n] Department of Pharmaceutical Nanotechnology, School of Pharmacy, Mashhad University of Medical Sciences, Mashhad, Iran

ARTICLE INFO

Article history:
Received 21 August 2017
Received in revised form
3 January 2018
Accepted 8 January 2018

Keywords:
Melanoma
Metastasis
Human adipose derived mesenchymal stem cells
CXCL10

ABSTRACT

Interferon γ-induced protein 10 kDa (IP-10) is a potent chemoattractant and has been suggested to enhance antitumor activity and mediate tumor regression through multiple mechanisms of action. Multiple lines of evidence have indicated that genetically-modified adult stem cells represent a potential source for cell-based cancer therapy. In the current study, we assessed therapeutic potential of human adipose derived mesenchymal stem cells (hADSC) genetically-modified to express IP-10 for the treatment of lung metastasis in an immunocompetent mouse model of metastatic melanoma. A Piggybac vector encoding IP-10 was employed to transfect hADSC *ex vivo*. Expression and bioactivity of the transgenic protein from hADSCs expressing IP-10 were confirmed prior to *in vivo* studies. Our results indicated that hADSCs expressing IP-10 could inhibit the growth of B16F10 melanoma cells and significantly prolonged survival. Immunohistochemistry analysis, TUNEL assay and western blot analysis indicated that hADSCs expressing IP-10 inhibited tumor cell growth, hindered tumor infiltration of Tregs, restricted angiogenesis and significantly prolonged survival. In conclusion, our results demonstrated that targeting metastatic tumor sites by hADSC expressing IP-10 could reduce melanoma tumor growth and lung metastasis.

* Corresponding author. Biotechnology Research Center, Pharmaceutical Technology Institute, Mashhad University of Medical Sciences, P.O. Box: 91779-48564, Mashhad, Iran.
** Corresponding author. Department of Genetics and Molecular Biology, School of Medicine, Isfahan University of Medical Sciences, Isfahan, Iran.
*** Corresponding author. Nanotechnology Research Center, Pharmaceutical Technology Institute, Mashhad University of Medical Sciences, Mashhad 91775-1365, Iran.
E-mail addresses: sahebkara@mums.ac.ir, amir_saheb2000@yahoo.com (A. Sahebkar), r_salehi@med.mui.ac.ir (R. Salehi), Jafarimr@mums.ac.ir (M.R. Jaafari).

https://doi.org/10.1016/j.canlet.2018.01.029
0304-3835/

1. Introduction

Melanoma is known as a metastatic and aggressive type of cancer that in most cases is diagnosed in the late stages [1]. It has been shown that melanoma cells have preferential metastasis to the lung, brain, skin, and liver tissues [2,3]. Therefore, finding a new effective treatment for patients with metastatic melanoma is necessary.

CXCL10 (also known as interferon-inducible protein (IP-10)) is an important CXC chemokine which possesses various anti-cancer effects [4,5]. IP-10 shows anti-angiogenic and apoptotic effects on various cancer cells [5]. It has been shown that this chemokine could contribute to the generation and trafficking of activated T cells to the inflammation and tumor sites and improve immune system against tumor cells [6–8]. Hence, it seems that IP-10 could be used as a therapeutic option for the treatment of various types of cancer including melanoma. Several studies have employed immunotherapy-based approaches against different targets for the treatment of patients with melanoma [9,10]. However, utilization of these approaches is associated with some limitations and adverse effects. Hence, specific targeting of immunomodulatory factors such as cytokines and chemokines could overcome these limitations [9,10].

Multiple lines of evidence have indicated that mesenchymal stem cells (MSCs) could migrate to tumor sites *via* expressing various receptors (e.g. CCR1, CCR2, CCR5, CCR6 and CXCR1), growth factors (e.g. TGF-β1, PGF, and HGF) and other proteins (antigen 4, and vascular cell adhesion molecule-1) [11]. Therefore, these cells could be applied as a cellular vehicle for carrying various therapeutic agents [12–15]. Adipose tissue is one of the important sites for the isolation of MSCs [16]. Several studies have confirmed that ADSCs could be an efficient vehicle for the delivery of different therapeutic agents to tumor sites [15,16].

In the current study, we assessed the therapeutic effect of human adipose-derived mesenchymal stem cells (hADSCs) expressing IP-10 in a melanoma lung metastasis model.

2. Material and methods

2.1. Isolation of hADSCs and culture

Human adipose tissues were provided from lipoaspirate samples of abdominal fat from male donors (age range 20–30 years) and after obtaining informed consent and were split as previously described [17]. At first, to remove contaminating debris and red blood cells of adipose tissue samples, they were washed with phosphate-buffer saline (PBS). Samples were treated with 0.075% collagenase type I in PBS for 30 min at 37 C. For neutralization of enzyme activity were added an equal volume of Dulbecco's modified eagles medium (DMEM/F12) (Gibco BRL, Paisley, UK) containing 10% fetal bovine serum (FBS). The reached infranatant was centrifuged for 10 min at 1,2009g and cellular pellet was resuspended in specific media (DMEM/F12, 10% FBS, and 1% penicillin/streptomycin). These cells were split in 25 cm2 flasks for 4–5 days in a 37 C humidified incubator with a 5% CO2 environment to provided good confluency (80%) (These cells defined as passage 0). At good confluency, cells were split with 0.25% Trypsin/0.02% EDTA at the ratio of 1:3 in every passage. Moreover, all procedures were approved by the Ethics Committee of Mashhad University of Medical Sciences.

2.2. Immunotyping of ADSCs

Immunotyping of ADSCs was performed by flow cytometry on a FACscan flow cytometry in our previous study (Becton–Dickinson, San Jose, CA). Briefly, a total of 5×10^5 human ADSCs (within 3 passages) were provided by trypsinization, and washed with 1% BSA/PBS. At other step, the reached cells were incubated with antibodies against human CD90, CD44, CD14, and CD45 (Chemicon, Temecula, CA, USA) for 30 min at 4 °C. Analysis of the FACS data was carried out with a FlowJo software version 10 (Treestar, OR).

2.3. Plasmid construction

Plasmid pCMV-hyPBase was obtained from the *Wellcome Trust Sanger Institute* (Hinxton, Cambridge, UK). The coding sequence of Piggybac transposase was amplified by Pfu polymerase using 5′-ATATACGCGTTGACATTGATTATTGACTAG-3′ and 5′-ATTGCTAG-CAGCTGGTTCTTTCCGCCTC-3′ as forward and reverse primers, respectively. Then it was cloned into Mlul and Nhel restriction sites of pPIG- IP-10 (CXCL10). Synthesized pPIG- IP-10 plasmid is composed of coding sequence of mouse IP-10 and hygromycin resistance genes separated by 2A peptide sequence. Theses coding sequences are flanked by terminal repeat element (TRE) sequence of Piggybac (Fig. 1A).

We used other Piggybac vectors including pT-tdTomato, pT-neo and pTrans For transfection of B16f10 cell lines (kindly provided by Dr. Masahiro Sato) (Fig. 1 B). These vectors were created by standard cloning procedures. Briefly, the pPB vector consists of two PB acceptors with inverted repeats. pT-neo (formerly referred to as pTpB) is a pPB-based vector which is consisted of a neomycin resistance gene (*neo*) expression unit (CMV promoter + *neo* + poly(A) sites). pT-tdTomato is a pPB-based vector which is consisted of a tandem dimer Tomato (*tdTomato*) cDNA expression unit under the control of the CAG promoter. Moreover, the pTrans vector expresses transposase under the CAG promoter [18].

2.4. Human ADSCs transfection, selection, and transgene expression

ADSCs cells were transfected by the Lipofectamine 2000 transfection reagent (Invitrogen, CA, USA). 5×10^6 ADSCs were plated in a 6-well plate to obtain a confluency of 80% after 24 h. *Transfection* efficiency was assessed using a helper-independent plasmid. *Forty-eight hours after transfection,* cells were treated with 150 μg/mL of hygromycin B (Roche) to allow the growth of stable clones for at least 14 days.

2.5. Cancer cell culture, transfection, and selection

The B16F10 cell line was purchased from the Pasteur Institute of Iran (https://www.pasteur.fr/en). Cancer cells were maintained in cellular medium at 37 °C in a 5% CO2 atmosphere. In the present study, B16F10 was transfected with pT-tdTomato, pT-neo and pTrans to provide RFP-melanoma cells respectively (Fig. 2). Lipofection was used for modification of melanoma cells. Briefly, to provide transgenic B16F10 cells, a density of 2×10^5 cells per well in triplicate for each group was seeded in 6-well plates. After 24 h, cells were co-transfected with the vector pT-tdTomato, pT-neo and pTrans using lipofectamine 2000™ transfection reagent (Invitrogen, Carlsbad, CA) according to the manufacturer's instructions. We checked transfection cells 24 h, 48 h and 72 h after transfection. Melanoma cells were selected, and maintained with 1000 μg/mL of G418. RFP melanoma was exposed to 400 μg/mL neomycin (Invitrogen, Carlsbad, CA) for about two weeks.

2.6. Reverse-transcriptase polymerase chain reaction (RT-PCR)

To confirm the up-regulation of IP-10 gene expression in hADSCs, total RNAs were isolated from the hADSCs and reverse

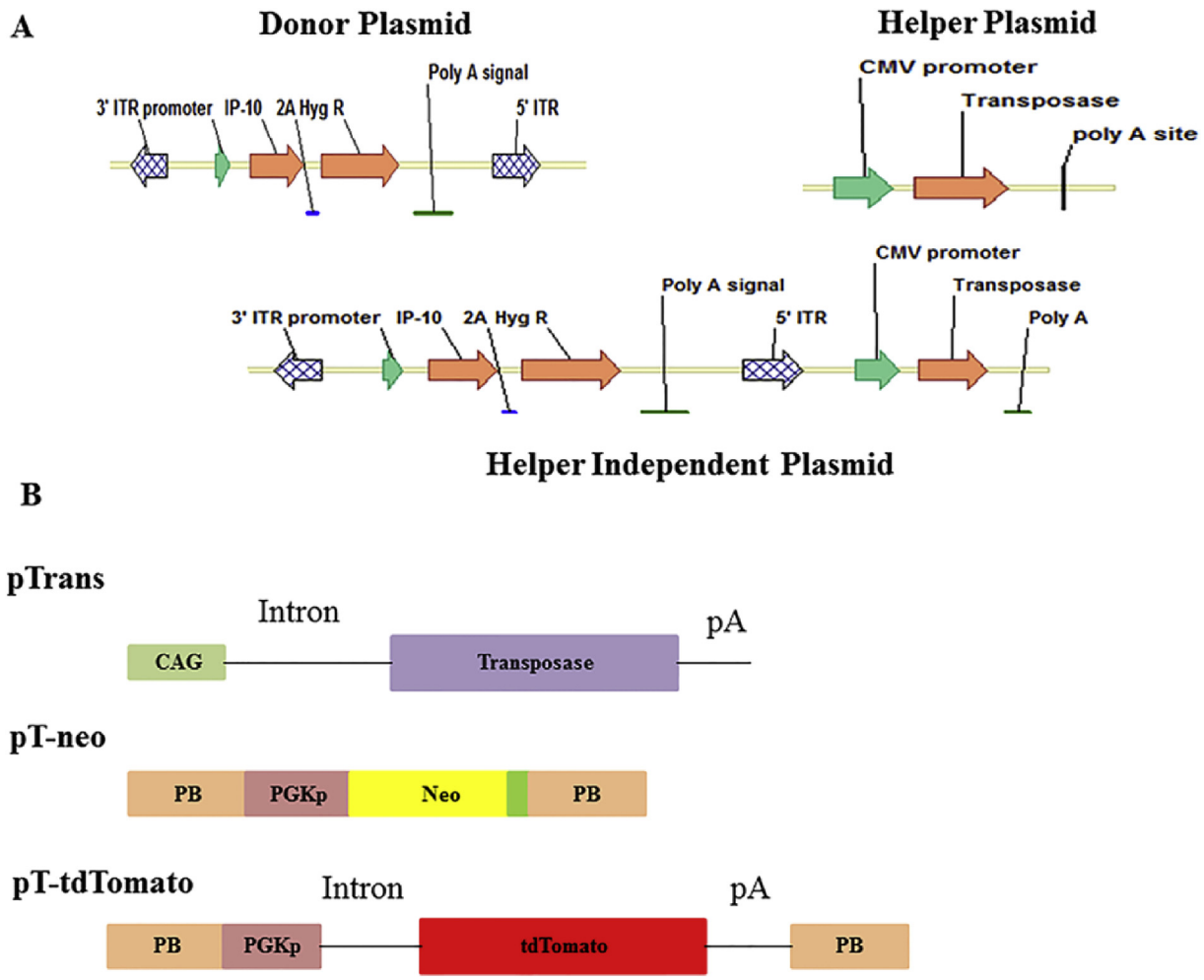

Fig. 1. Schematic presentation of the used vectors for transfection of hADSCs and B16F10. Here briefly describe what is shown in the figure. The plasmid backbone is not shown in the figure. A) Piggybac containing IP-10 and EGFP. ITR: Inverted Terminal Repeat; IP-10: Interferon gamma-induced protein 10; Hyg R: ***Hygromycin resistance***; ***CMV:*** cytomegalovirus. B) Depiction of the expression vectors used for transfection of melanoma cells. The plasmid backbone is not shown in the figure. CAG: cytomegalovirus enhancer 1 chicken b-actin promoter; pA: poly (A) sites; neo: neomycin resistance gene; PB: acceptor site in the PiggyBac system; PGKp: mouse phosphoglycerate kinase promoter; tdTomato: tandem dimer Tomato cDNA; Transposase: PB transposase gene.

transcription-PCR (RT-PCR) was performed as described previously (64). The PCR primer sequences targeting murine IP-10 were forward 5′-CGGAATTCATCAGCACCATGAACCCAAGT-3′, and revers 5′-GCGTGGCTT CTCTCCAGTT-3′, and GAPDH forward 5′-CTGCACCAC-CAACTGCTTAG-3′) and revers 5′- GTCTGGGARGGAAARRGRGA-3'.

2.7. Western blot on cultured cells

To analyze the expression of IP-10 in hADSCs, Piggybac-IP-10 (PB-IP-10) was transfected by Lipofectamine 2000 to hADSCs in culture. After 48 h, all groups of hADSCs were lysed in lysis buffer (10 mM Tris-Cl, pH 7.4, 0.15 M NaCl, 5 mM EDTA, and 1% Triton X-100) containing 100 g/mL protease inhibitors (Sigma-Aldrich, St. Louis, http://www.sigmaaldrich.com). The content of IP-10 was determined using the Bio-Rad Dc protein assay kit (Bio-Rad, Mississauga, ON, Canada). Ten micrograms of total protein from each sample was separated by 10% SDS-polyacrylamide gel electrophoresis and *trans*-blotted onto polyvinylidene difluoride membrane. The membranes were blocked in blocking buffer (5% powdered non-fat milk in PBS) containing 0.05% Tween-20. The blot was probed with a polyclonal rabbit anti-mouse IP-10 antibody at 1:1000 (catalog no. ab9938; Abcam, Cambridge, MA) followed by binding with an anti-rabbit secondary antibody at 1:11000 dilution (catalog no. ab37168; Abcam, Cambridge, MA). IP-10 protein and GADH (control) bands was identified using chemiluminescence kit (Amersham Biosciences/GE Healthcare, Little Chalfont, U.K.,).

2.8. Cell proliferation assay

Melanoma cells were seeded in 96-well plates at a density of 7.5×10^3 cells per well and incubated at 37 °C for 24 h. Supernatants from mock and IP-10 plasmid transfected hADSCs were added to the plate and returned to the incubator for 3 days. We determined IP-10 concentration using ELISA at about 2.4 ng/mL of supernatant. 3-(4,5-Dimethylthiazol-2-yl)-2,5-diphenyltetrazolium bromide (MTT) dye was added to each well for 4 h. The reaction was stopped by addition of dimethyl sulfoxide (DMSO). Optical density was measured at 570 nm (and 670 nm for background) in a multi well plate reader (model 3550; Bio-Rad). Background absorbance of the medium in the absence of cells was subtracted. In this study, samples were treated in triplicate, and the mean for each experiment was calculated. Results were considered as a percentage of the untreated control, which was defined as 100%. Experiments were repeated at least three times and the mean IC50 value

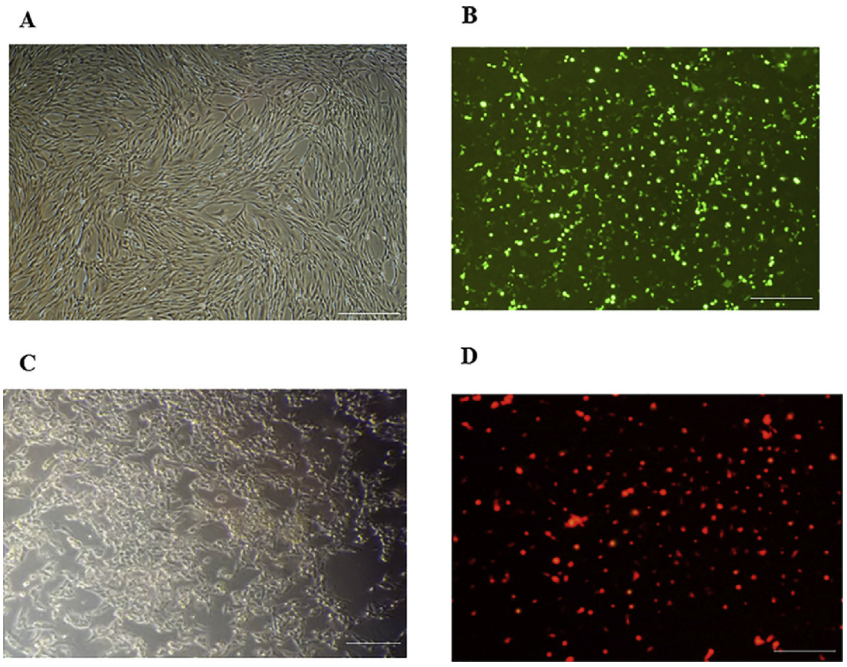

Fig. 2. Piggybac-based gene delivery generates stable transfectants derived from hADSCs and B16F10. A) Untranfected hADSCs, B) Transfected hADSCs containing EGFP, C) Untranfected B16F10, D) Transfected B16F10 containing RFP (tdTomato). Bar = 100 μm.

standard deviation was determined by Graphpad Prism.

2.9. In vivo studies

Eight-week-old female C57BL/6 mice were purchased from the Pasteur institute of Iran. Maintaining of the animals was done in accordance with Institutional Animal Care and Use Committee guidelines. Each group included 20 mice (10 mice for laboratories tests and 10 mice for survival), and the experiment was repeated twice. For establishing lung metastasis, 3×10^5 B16F10 cells were injected by tail vein into each mouse. After 10 days, tumors established in the lungs and mice were tail vein injected with 1×10^6 cells of three different hADSCs groups: unmodified hADSCs, hADSCs-mock and hADSCs expressing IP-10. To confirm the establishment of tumors in the lungs we used transfected REF-B16F10 and to track hADSCs we used hADSCs-EGFP (the main vector composed of IP-10 + EGFP).

Mice were euthanized at different time points; tissue samples were harvested, and were made paraffin sections from each sample. Tissue sections were dewaxed by xylene and rehydrated in graded alcohol. Endogenous peroxidase activity was blocked with 0.3% (vol/vol) hydrogen peroxide in methanol before the slides were washed in water. Slides were incubated in citrate buffer (pH 6.0) for 20 min in a steamer for antigen retrieval for anti-CD31, anti-CD137, and anti-Foxp3. Nonspecific binding was blocked by incubating the slides in 5% (vol/vol) in normal serum (depending on the animal in which the secondary antibody was raised). The following primary antibodies, at the following dilutions, were used: anti-CD31, 1:50 dilution (catalog no. ab28364, Abcam; Cambridge, MA); anti-CD137 polyclonal antibody, 1:600 dilution (catalog no. ab203391, Abcam; Cambridge, MA); and antibody for anti-F0xp3, 1:100 dilution (catalog no. ab54501; Abcam, Cambridge, MA). After binding primary antibodies, slides were incubated with the respective secondary antibodies conjugated to horseradish peroxidase, 1:1000 dilution (catalog no. ab97200; Abcam, Cambridge, MA). The bound antibody was visualized by the peroxidase-based Vectastain Elite ABC Kit (Vector Laboratories, Peterborough, UK). The substrate reaction was stopped by washing the slides in running water. Finally, the slides were lightly counterstained with hematoxylin. To investigate the cell apoptosis, the tissue sections were treated with the DAB (3, 3-diaminobezidine tetrahydrochloride) (Roche Applied Science, Mannheim, Germany) substrate solution for color development in a dark chamber at room temperature for 10 min. After dehydration of tissue sections in ethanol, they were cleared by xylene, and mounted by DPX (Shandon, Thermo scientific, USA). Finally, tissue sections were evaluated by fluorescent microscope under ×100 eyepiece magnification in each sample. To determine total number of cells and the number that stained positive in each field, 10 randomly chosen fields were counted [12].

2.10. Enzyme-linked immunosorbent assay

Blood was collected from mice at different time points (before and after treatment), and serum was maintained frozen at 80 °C. To quantitate the amount of IP-10 protein, serum was applied in triplicate in an enzyme-linked immunosorbent assay (ELISA) specific for mouse IP-10 (catalog no. ab9938; Abcam, Cambridge, MA) according to the manufacturer's protocol and analyzed at an absorbance of 450 nm.

2.11. Western blotting on mouse tissues

Western blotting was applied to investigate *in vivo* apoptosis and homing of hADSCs in 10 samples of fresh lung tissue in various groups. A measured amount of proteins were separated by SDS-PAGE and transferred to membranes. The membranes were blocked with 5% non-fat dry milk in TBST buffer for 2 h at room temperature, treated with anti-caspase 8 antibody (catalog no. 9746; Cell Signaling, USA), 1:1000 dilution overnight at 4 °C, washed in TBST, and treated again with horseradish peroxidase-conjugated secondary antibody 1:1000 dilution (catalog no. ab37168; Abcam, Cambridge, MA) for 2 h at room temperature. Enhanced chemiluminescence was used to determine protein

immunoreactive. Survival analysis was done on 10 mice in the each group. The time to reach end point (TTE) for each mouse was assessed based on the equation of the line reached by exponential regression of the tumor growth curve. The percent of tumor growth delay (%TGD) was obtained from the equation %TGD = (T - C)/C × 100 based on the difference between the mean TTE of various group (T) and the mean TTE of the control group (C) [19]. Increase life span (%ILS) for each group was assessed based on the following equation: (mean survival time of each group/mean survival time of control group × 100) - 100 [20].

2.12. Terminal deoxynucleotidyl transferase-mediated dUTP nick-end labeling (TUNEL) assay

To assess apoptosis, we used TUNEL assay. Samples were prepared as described above [21]. At first, tissue samples from lung were fixed in 10% neutral buffered formalin solution, and embedded in paraffin**.** The presence of apoptotic cells within the tissue samples was performed using the *in situ* cell death detection kit (Fluorescein; Roche) following the manufacturer's instructions. It is based on the enzymatic addition of digoxigenin nucleotide to the nicked DNA by terminal deoxynucleotidyl transferase. In the tissue sections, ten equal-sized fields were randomly chosen and analyzed.

2.13. Statistical analysis

Statistical analysis was done using SPSS version 19 (SPSS Inc, Chicago, IL). The statistical differences between the groups were performed by Student *t*-test, ANOVA, and log-rank tests. Survival was defined as the date of melanoma cell injection to the date of death. *P* values less than 0.05 were considered statistically significant**.**

3. Results

3.1. Expression of EGFP and RFP in hADSCs and B16F10

Characterization of hADSCs was done in our previous study [17]. To evaluate the efficiency of the Piggybac system in generating stable transfectants, hADSCs and B16F10 cells were transfected with one and three vectors, respectively, and transfection efficiency was assessed using fluorescent microscope 72 h after transfection. Our results indicated that transfection rate in hADSCs and B16F10 cells were 95–100% (Fig. 2). Transfection rates were determined by counting the number of hADSCs containing EGFP and B16F10 containing tdTomato in 10 randomly chosen areas of cell culture. Moreover, we obtained stable clones of transfection cells through treating hADSCs and B16f10 cells with hygromycin B and neomycin for at least 14 days respectively.

3.2. High level expression and bioactivity of piggybac encoding IP-10

High expression of the transgenic mRNA and protein was confirmed using RT-PCR and Western blot analyses, respectively. hADSCs were transfected with either mock or PB-IP-10. Fig. 3A and B shows a strong band of IP-10 in the PB-IP-10 group but not in the control group (mock), which confirmed high-level expression of the transgenic protein at the expected molecular weight of 8.7 kDa [22].

To determine the bioactivity of PB-IP-10 transgene protein, hADSCs were either transfected with mock or PB-IP-10. One week later, supernatants were harvested and concentrated. IP-10 concentration in the supernatant was assessed using ELISA and found to be 2.4 ng/mL. To investigate the effects of IP-10 on cell proliferation, MTT assay was performed in B16F10 cells. The results showed significant inhibition of tumor growth with 100 μl of supernatant from hADSCs transfected with PB-IP-10 ($p < 0.001$; Fig. 3C).

3.3. MSC homing to tumors in the lung and expressing IP-10

To determine tumor establishing in the lungs, we used B16F10 transfected with PB– tdTomato (RFP). After 10 days, tumors were established in the lungs. To assess the homing of transplanted hADSCs to tumor sites in the lungs, we injected hADSCs-IP-10 which also expressed EGFP. The modified B16F10 and hADSCs were intravenously injected to mice. Ten days after the administration of hADSCs, the mice were sacrificed and tissues were harvested. Microscopic and western blot analysis of mice lung provided evidence that tumors had manifested in lungs and homing of hADSCs to the tumor site in the lungs as shown in Fig. 4. Systemic expression of IP-10 in mice that received hADSC was also confirmed by ELISA on serum of mice in specific time points. Our results indicated that there was no significant increase in the level of IP-10 after treatment in the hADSCs expressing IP-10 group than other groups ((*, $p < 0.05$) **(**Fig. 4D**).**

3.4. Antitumor effects of hADSCs transfected with a PB-IP-10

One hundred C57BL/6 mice divided in five groups (20 mice per group) and 3×10^5 B16F10 cells were injected by tail vain. After ten days, mice were received no treatment or hADSCs (1×10^6) that were without vector or with mock or PB-IP-10. Twenty day later, ten mice in each group were sacrificed to assessing the effect of therapy, and the remaining mice ($n = 10$) were considered for long-term survival (Fig. 5). Our results indicated that treatment of B16F10 bearing mice with hADSCs expressing IP-10 could significantly decrease metastatic colonies in the lungs ($p < 0.001$)(Fig. 5 A, B, Table 1). There was no significant therapeutic effect observed in other groups (Fig. 5B). hADSCs expressing IP-10 were observed to significantly increase the survival of mice. Whereas all animals in control group died by day 30, more than 80% of mice given hADSCs expressing IP-10 survived beyond that time ($p < 0.01$)(Fig. 5C). Survival of 30% mice in hADSC-IP-10 group was found up to 70 days. Table 1 provided some key indicators which are associated with therapeutic efficacy on various groups including median survival time (MST), time to reach end point (TTE), tumor growth delay (%TGD), and increase life span (%ILS) for each treatment group in mouse model. The hADSC-IP-10 group significantly increased the MST, TTE, TGD and ILS compared to all the other groups. However, there were no significant differences among No treatment group (B16F10), control PBS, hADSC, hADSCs + Mock.

3.5. Effects of hADSCs –IP-10 on apoptosis, and angiogenesis

Results of immunohistochemistry, TUNEL assay, Western blotting and the quantitative analysis showed a significant decrease in tumor vasculature ($p < 0.01$) and an increase in apoptosis ($p < 0.01$) following treatment with hADSCs producing IP-10 compared with untreated animals. No such a difference versus control group was seen in tumors of mice treated with other groups which suggested that the effects were due to IP-10 (Fig. 6).

3.6. Effects of hADSCs transfected with a PB-IP-10 on immune cells (activated T cells and Tregs)

We have assessed the activation and infiltration of T cells and Tregs in the lung after injection of hADSCs-IP-10 compared with hADSCs, hADSCs-mock, and PBS groups (Fig. 7). Results of

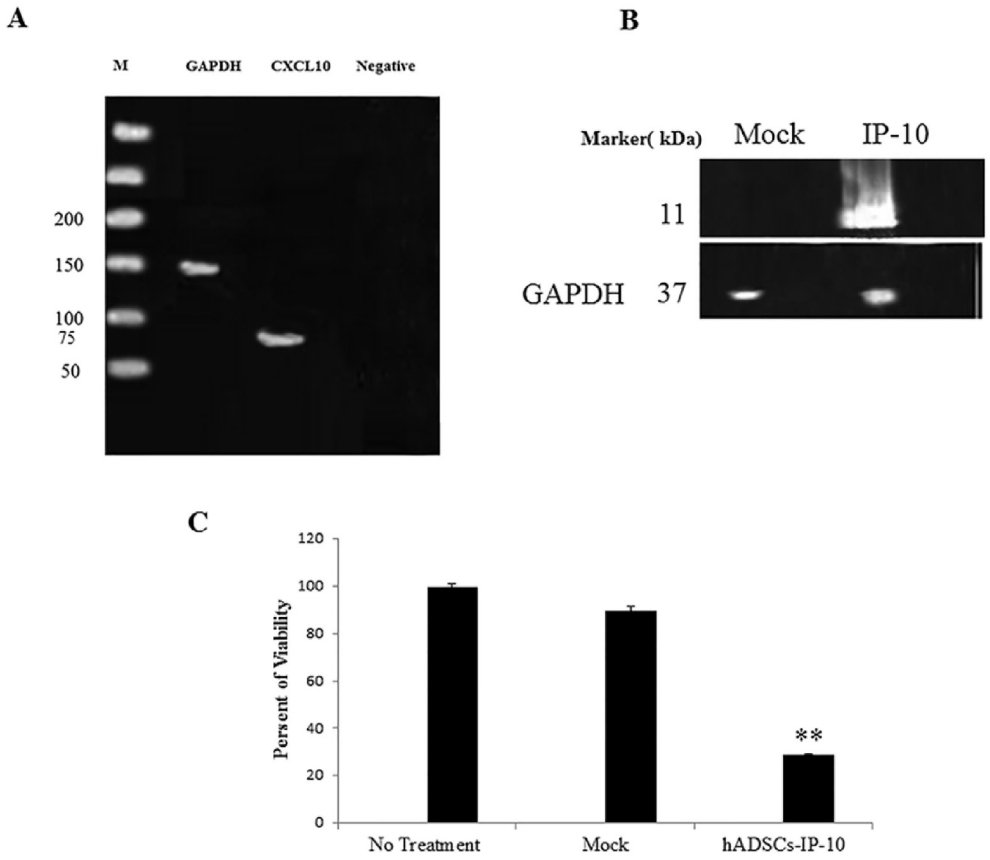

Fig. 3. Expression of IP-10 in hADSCs was analyzed by RT-PCR (A) and Western blot (B) following transfection with PB- IP-10 or mock. The effect of PB- IP-10 on cell proliferation is shown in (C). The bioactivity of PB-IP-10 was determined *in vitro* in B16F10 cells by incubating the cells in conditioned media obtained from hADSC cultures which were either transfected, mock or PB-IP-10 (**, $p < 0.001$). Error bars represents (e.g. standard deviation).

immunohistochemistry and Quantitative analysis indicated that there are significant difference in population of activated T cells and Tregs between hADSCs-IP-10 and other groups respectively (***, $p < 0.001$).

4. Discussion

For many years, the cornerstones of cancer therapy has been surgery, chemotherapy and radiotherapy [23]. Over the last decade, targeted therapies have emerged as promising treatments for various types of cancer. Furthermore, current limitations in the conventional therapies for solid and metastatic tumors such as systemic toxic side effects and insufficient accumulation of therapeutic agents in the tumor sites preclude achieving complete remission in most patients [23]. Therefore, there is a need to find alternative treatments that can circumvent the challenges posed by the current conventional anticancer therapies. One approach for cell based-cancer therapy involves the use of genetically-engineered MSCs [24,25]. Tumor microenvironment provides a preferential niche for MSCs homing to tumor sites. As such, inherent tumor-tropic properties of MSCs makes them appealing candidates for targeted delivery of anticancer agents [24,26,27].

One of the chemoattractant cytokine with pleiotropic antitumor effects is IP-10 [4]. IP-10 displays several anticancer effects including induction of tumor cell necrosis, generation of effector T cells, attraction of T cells, monocytes, neutrophils, and possibly NK cells to tumor sites, restriction of tumor angiogenesis and inhibition of metastasis [4]. In this regards, it seems that generation of genetically-modified MSCs producing IP-10 has a great therapeutic potential in the treatment of cancers particularly metastatic tumors. In the current study, we evaluated the antitumor activity of IP-10-producing hADSCs in an immunocompetent mouse model of metastatic melanoma. Our results indicated that hADSCs were able to deliver IP-10 to primary and metastatic tumor sites *in vivo*. Several studies have demonstrated that injection of autologous *ex vivo*-expanded MSCs alone or in combination with various therapeutic agents is associated with relatively benign adverse effects in cancer patients [13,14,28–31]. We found that there was no specific immune response against the injected cells, explaining not only the prolonged survival of MSC in our model but also the immunomodulating effect of our therapeutic strategy. In agreement with our findings, previous studies showed that allogeneic MSCs did not elicit specific cellular immune response against the transplanted cells [32–34]. Grisendi et al. demonstrated that hADSCs producing tumor necrosis factor–related apoptosis-inducing ligand (TRAIL) engrafted into tumors mediated apoptosis without a significant toxicity to normal tissues. They concluded that transgenic hADSCs could be used as safe cellular therapeutic vehicles for cancer therapy [16]. In another study, we used hADSCs producing IFNγ in an immunocompetent mouse model of metastatic melanoma [15]. Our *in vivo* results showed that IFNγ-expressing ADSCs, localized into tumor stroma, inhibited tumor growth and angiogenesis, hindered systemic increase of Tregs, enhanced expression of PD-L1 and infiltration of $CD8^+$ cells (but not interleukin-2+ cells), and prolonged the survival of mice [15].

In the current study, we showed that there was no significant increase in the serum level of IP-10. A large number of studies have indicated that elevated serum levels of various cytokines are

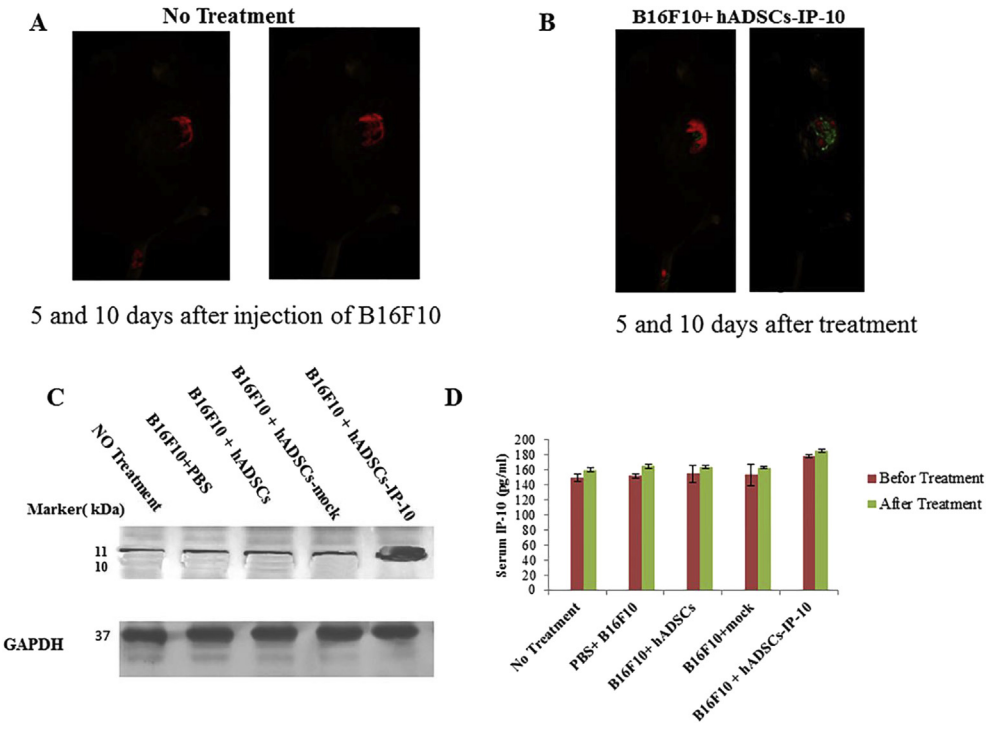

Fig. 4. Tumor establish and homing of hADSC in mice lungs. Microscopic analysis of establishing B16F10 in lungs and the homing of hADSCs expressing IP-10 in tumor sites in lungs, confirmation of expression of IP-10 in lungs and systemic IP-10 levels before and after treatment. C57BL/6 mice bearing B16F10 -tdTomato tumors ($n = 20$) in the lungs were injected with 1×10^6 hADSCs expressing IP-10. Tumor establishment was defined 6 days after injection and homing of hADSCs expressed IP-10 were defined in ten days after treatment by microscopic (A,B) and western blot analysis (C). Twenty days after injection, mice were sacrificed, lungs were harvested, and samples were provided for Western blotting (C). An ELISA for IP-10 levels was done in triplicate with serum samples from mice in before and after treatment with hADSCs (D). Error bars represents (e.g. standard deviation).

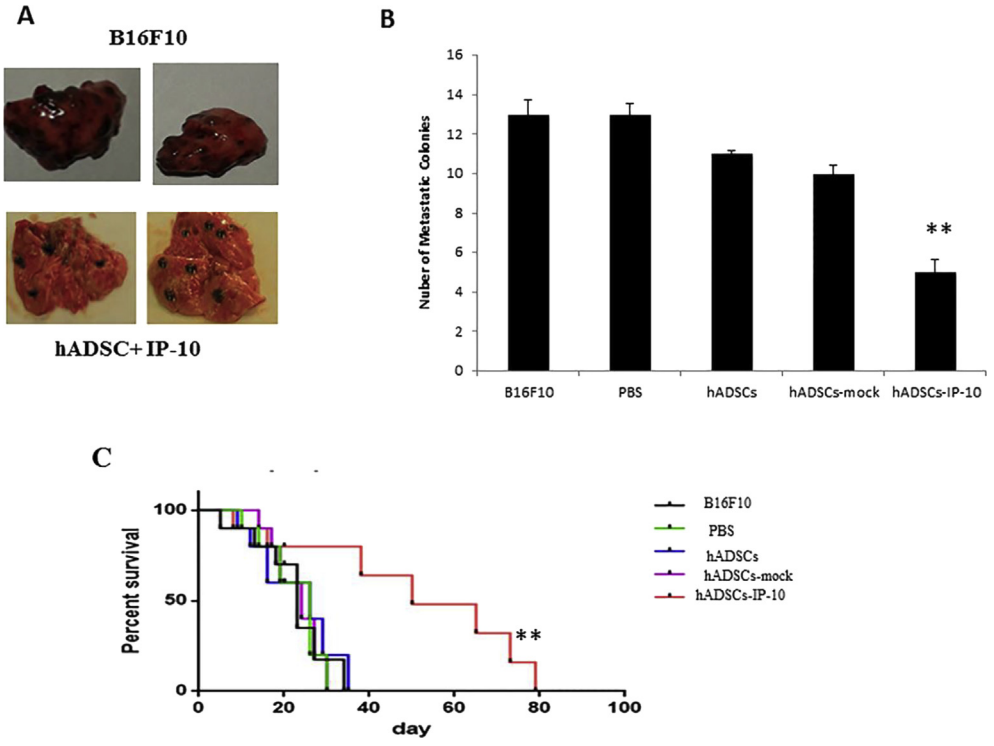

Fig. 5. In vivo experiment. C57BL/6 mice were injected with 3×10^5 B16F10 cells by tail vein injection. After ten days, mice were treated with hADSCs (1×10^6 cells). Mice were divided into five groups (each group 20 mice), which included no treatment, PBS, hADSCs, hADSCs-mock and hADSCs-IP-10. Ten mice of each group were sacrificed at day 20 to determine the effect of therapy, and the remaining mice ($n = 10$) were allowed long-term survival. The *in vivo* experiment was repeated twice. Images represent a part of lungs from the indicated treatment groups on day 20 **(A)** and the number of metastatic colonies (**, $p < 0.01$) **(B)**. Survival index is shown in **(C)** (**, $P = .0366$). Error bars represents (e.g. standard deviation).

Table 1
Therapeutic efficacy data of various treated groups in mice bearing B16F10 metastatic lung tumor.

Group	MST (day)	TTE (days ± SD)	TGD (%)	ILS
B16F10	23	20.42 ± 1.56	–	
PBS	26	20.57 ± 2.85	0.73	13.04
hADSC	26	20.42 ± 1.26	–	–
hADSC + Mock	24	21.42 ± 4.31	4.89	4.34
hADSC-IP-10	50	47 ± 3.22	130.16	117.39

MST: Median survival time, TTE: Time to reach end point, TGD: Tumor growth delay, ILS: Increase life span.

associated with systemic adverse effects in patients. Therefore, it seems that employing hADSCs for delivering IP-10 to the tumor sites without significant increase in plasma cytokine level would prevent undesirable systemic adverse effect. According to our results, hADSCs expressing IP-10 are able to restrict the anti-cancer activity of IP-10 to tumor sites without evidence of systemic adverse effects. These results suggest that hADSCs could be used as effective vehicles for targeting therapeutic agents.

It has been shown that IP-10 can induce apoptosis in cancer cells. Our results indicated that hADSCs expressing IP-10 significantly increased apoptosis rate in melanoma cells. Western blotting for caspase 8 indicated that IP-10 exerts its pro-apoptotic effects likely *via* targeting caspase 8. Sahin et al. showed that CXCL10 mediated the apoptosis of hepatocytes through TLR4 signaling, a non-cognate chemokine pathway. Therefore, CXCL10 specifically induces prolonged protein kinase B and Jun N-terminal kinase activation, leading to hepatocyte apoptosis by caspase-8, caspase-3, and p21-activated kinase 2 (PAK-2) cleavage [35]. It has been exhibited that caspase-8 is an upstream caspase and could cleave its downstream molecules such as caspase-3 and PAK-2 in response to IP-10 [35,36].

Inhibition of angiogenesis is another important effect of IP-10 which contributes to tumor regression in various cancers such as melanoma. We showed that IP-10 is able to significantly decrease angiogenesis and vessel density in the metastatic lung tissue. Yates-Binder et al. demonstrated that utilization of an IP-10-derived peptide (IP-10p) significantly inhibited tube formation and VEGF-induced endothelial motility *in vitro, the properties* crucial for angiogenesis [37]. Moreover, an *in vivo* study showed that IP-10p is able to reduce both vessel formation and induced involution of nascent vessels through increasing cAMP production, activation of PKA and, thereby, inhibiting cell migration and VEGF-mediated *m*-calpain activation [37].

We showed that IP-10 increased the number of activated T cells but decreased Treg cells in the tumor tissue. Through interacting with tumor cells and tumor-associated stroma, T cells and Tregs are

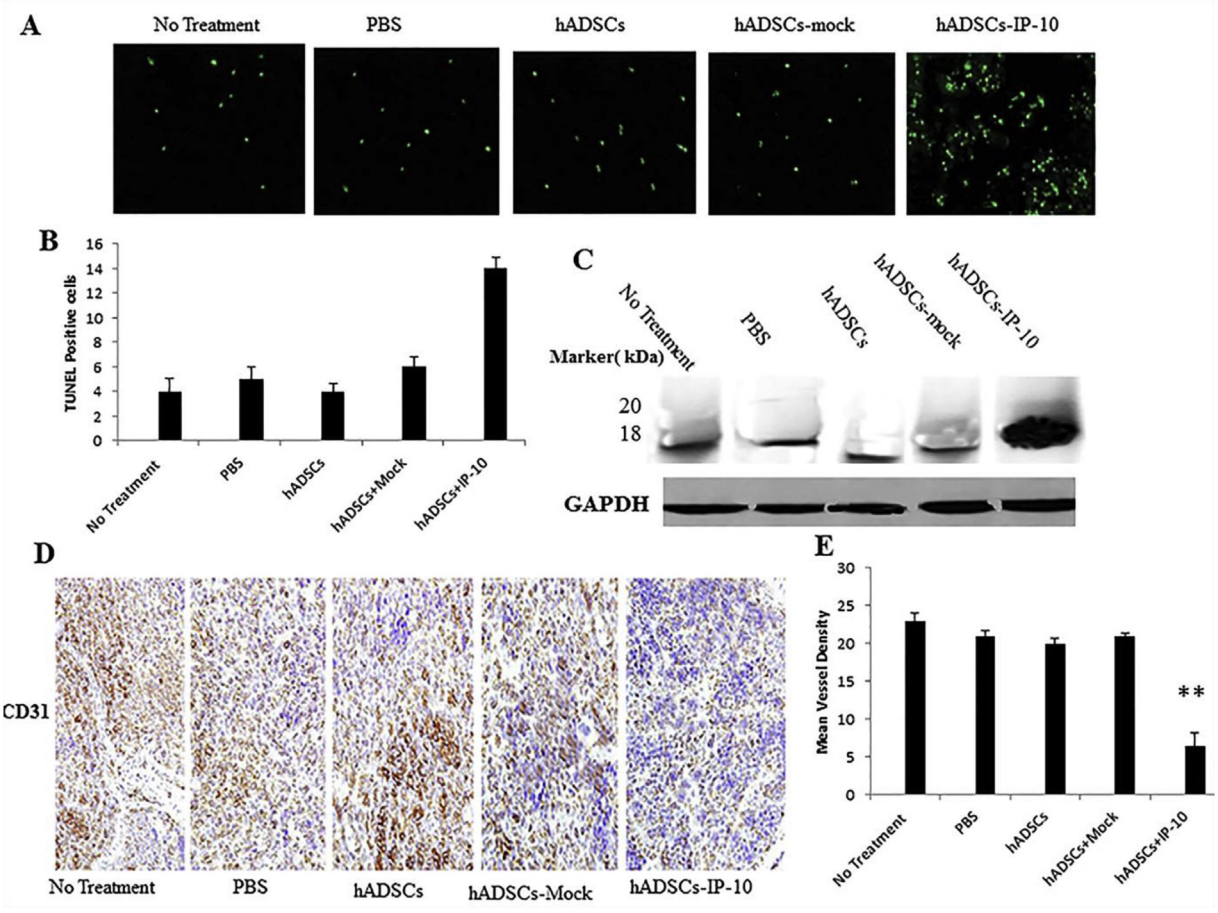

Fig. 6. TUNEL assay, western blotting, and immunochemistry of lungs with B16F10 tumors for assessing apoptosis, and angiogenesis. For immunochemical and TUNEL analysis of tumor cell apoptosis, and microvessel density, lungs were paraffin-embedded and sectioned. TUNEL assay was carried out in lungs sections treated with or without therapy after 10 days and fluorescence images were visualized under an Axio vision 4.0 fluorescence microscope (A). Quantitative analysis of apoptotic indices were calculated by counting positive cells in 10 random fields (** p 0.01) **(B).** Ten days after treatment, lungs were harvested, and samples were provided for Western blotting for Caspase 8 (C). Staining was performed with anti-CD31 polyclonal antibody for endothelial cells (D). Blood vessel counts were determined by counting the number of vessels in 10 randomly chosen areas of CD31 stained sections (** p 0.01) **(E).** Error bars represents (e.g. standard deviation).

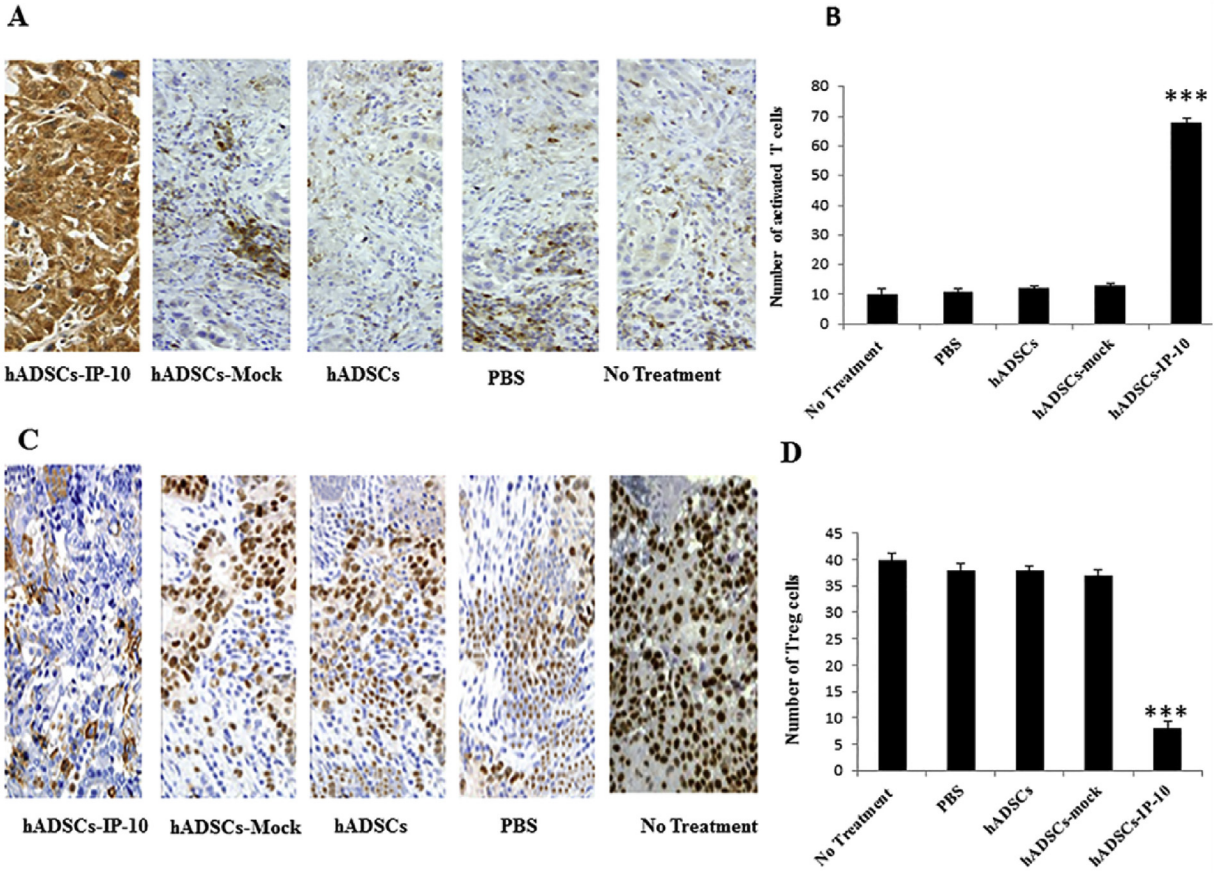

Fig. 7. Determination of immune cells (activated T cells and Tregs) in the lung following IP-10 therapy. All administrations were injected intravenously into C57BL/6 mice with lung metastases of B16F10 cells ($n = 20$ in each group). Twenty days later, lung was harvested; frozen sections were made the tissue for immunohistochemistry. Staining was done with rat polyclonal antibody specific for mouse CD137, and FOXP3. Slides were minimally counterstained with hematoxylin **(A, C)**. Quantitative analysis of activated T cells and Tregs were calculated by counting the number of cells in 10 randomly chosen areas of CD137 and FOXP3 stained sections respectively (***, p <0.01) ((B, D). Error bars represents (e.g. standard deviation).

key players in determining antitumor immune responses. Several studies have indicated that IP-10, either as combination therapy or stand-alone therapy, exerts its anti-tumor effects through multiple immunomodulatory mechanisms such as recruiting immature antigen-presenting cells or early activated T cells to the tumor site, promoting a strong CTL response, and suppressing Treg accumulation in experimental animal models [6,38,39]. It has also been shown that IP-10 can cause tumor necrosis and vascular damage at the tumor site without provoking a substantial inflammatory response [40]. Migration of T cells to the tumor site could enhance the therapeutic efficacy of the antitumor immune response. Sharma et al. demonstrated that some cytokines and chemokines including IFN-γ, CXCL9 and IP-10 exert their anti-tumor effects through increasing T cell populations (both $CD4^+$ and $CD8^+$) [7]. Dufour and colleagues reported that IP-10 can enhance generation and trafficking of activated T cells. In their study, IP-10 knockout (KO) mice showed a decreased recruitment of $CD4^+$ and $CD8^+$ lymphocytes accompanied by low levels of IFN-γ,CXCL9 and CXCL10 in the brain tissue.

Treg cells and their associated cytokines such as IL-10 and TGF-β may play a role in promoting tumor growth and progress by inhibiting the immune response against tumor. It has been shown that the number of Treg cells is inversely correlated with antitumor response of $CD8^+$ T cells and patients' survival [41–44]. In contrast to our results, various studies have revealed that tumor-derived IP-10 attracts Tregs to the tumor sites and thereby promotes immunosuppression and tumor progression. These studies suggested that IP-10 expression is correlated with Tregs infiltration and poor survival [45]-47). The dual effects of IP-10 (anti-tumor vs. tumorigenic effects) seem to be due to spliced variants of the corresponding CXCR3 receptor. It has been shown that CXCR3-B has growth-inhibitory effects, whereas CXCR3-A could induce cell proliferation (48).

In summary, our results demonstrated that hADSC-mediated delivery of IP-10 could induce apoptosis, increase trafficking of activated T cells to the tumor site, restrict angiogenesis, and hinder accumulation of Tregs in mice bearing melanoma lung metastasis. Moreover, our *in vivo* data indicated that employing hADSCs producing IP-10 could prolong survival of mice bearing B16F10 lung metastasis tumors. These findings suggest that hADSC-based targeted delivery of therapeutic agents such as IP-10 could be regarded as a novel and effective therapeutic strategy for inhibition of tumor growth and targeting tumor metastasis.

5. Acknowledgments

This study was supported by Biotechnology Research Center and Nanotechnology Research Centers of the Mashhad University of Medical Sciences (Mashhad, Iran) and Isfahan University of Medical Sciences (Isfahan, Iran). We would like to thank Dr Masahiro Sato at the Section of Gene Expression Regulation, Frontier Science Research Center, and Kagoshima University for providing the plasmids pT-tdTomato, pT-neo and pTrans.

References

[1] V. Gray-Schopfer, C. Wellbrock, R. Marais, Melanoma biology and new targeted therapy, Nature 445 (7130) (2007) 851–857.
[2] W. Kraybill, M. Mooney, Prognosis and staging of melanoma, Semin Oncol 23 (6) (1996) 725–733. Semin Oncol. 1997 Dec;24(6):756–757.
[3] M. Avril, P. Charpentier, A. Margulis, J. Guillaume, Regression of primary melanoma with metastases, Cancer 69 (6) (1992) 1377–1381.
[4] F. Antonicelli, P. Bernard, CXCL10 (Chemokine (CXC Motif) Ligand 10), 2012.
[5] M. Liu, S. Guo, J.K. Stiles, The emerging role of CXCL10 in cancer (Review), Oncol Lett. 2 (4) (2011) 583–589.
[6] X.B. Jiang, X.L. Lu, P. Hu, R.E. Liu, Improved therapeutic efficacy using vaccination with glioma lysate-pulsed dendritic cells combined with IP-10 in murine glioma, Vaccine 27 (44) (2009) 6210–6216.
[7] S. Sharma, S.C. Yang, S. Hillinger, L.X. Zhu, M. Huang, R.K. Batra, et al., SLC/CCL21-mediated anti-tumor responses require IFNgamma, MIG/CXCL9 and IP-10/CXCL10, Mol Cancer 2 (2003) 22.
[8] J.H. Dufour, M. Dziejman, M.T. Liu, J.H. Leung, T.E. Lane, A.D. Luster, IFN-gamma-inducible protein 10 (IP-10; CXCL10)-deficient mice reveal a role for IP-10 in effector T cell generation and trafficking, J. Immunol. 168 (7) (2002) 3195–3204.
[9] C. Franklin, E. Livingstone, A. Roesch, B. Schilling, D. Schadendorf, Immunotherapy in melanoma: recent advances and future directions, Eur. J. Surg. Oncol. 43 (3) (2017) 604–611.
[10] M. Khattak, R. Fisher, S. Turajlic, J. Larkin, Targeted therapy and immunotherapy in advanced melanoma: an evolving paradigm, Ther Adv Med Oncol 5 (2) (2013) 105–118.
[11] H. Mirzaei, A. Sahebkar, A. Avan, M.R. Jaafari, R. Salehi, H. Salehi, et al., Application of mesenchymal stem cells in melanoma: a potential therapeutic strategy for delivery of targeted agents, Curr. Med. Chem. 23 (5) (2016) 455–463.
[12] C. Ren, S. Kumar, D. Chanda, J. Chen, J.D. Mountz, S. Ponnazhagan, Therapeutic potential of mesenchymal stem cells producing interferon-alpha in a mouse melanoma lung metastasis model, Stem Cell. 26 (9) (2008) 2332–2338.
[13] M. Studeny, F.C. Marini, R.E. Champlin, C. Zompetta, I.J. Fidler, M. Andreeff, Bone marrow-derived mesenchymal stem cells as vehicles for interferon-beta delivery into tumors, Cancer Res. 62 (13) (2002) 3603–3608.
[14] M.R. Loebinger, A. Eddaoudi, D. Davies, S.M. Janes, Mesenchymal stem cell delivery of TRAIL can eliminate metastatic cancer, Cancer Res. 69 (10) (2009) 4134–4142.
[15] V. Bahrambeigi, N. Ahmadi, S. Moisyadi, J. Urschitz, R. Salehi, Haghjooy Javanmard S. PhiC31/PiggyBac modified stromal stem cells: effect of interferon gamma and/or tumor necrosis factor (TNF)-related apoptosis-inducing ligand (TRAIL) on murine melanoma, Mol Cancer 13 (255) (2014) 1476–4598.
[16] G. Grisendi, R. Bussolari, L. Cafarelli, I. Petak, V. Rasini, E. Veronesi, et al., Adipose-derived mesenchymal stem cells as stable source of tumor necrosis factor-related apoptosis-inducing ligand delivery for cancer therapy, Cancer Res. 70 (9) (2010) 3718–3729.
[17] N. Ghasemi, S. Razavi, M. Mardani, E. Esfandiari, H. Salehi, S.H. Zarkesh Esfahani, Transplantation of human adipose-derived stem cells enhances remyelination in lysolecithin-induced focal demyelination of rat spinal cord, Mol. Biotechnol. 56 (5) (2014) 470–478.
[18] E. Inada, I. Saitoh, S. Watanabe, R. Aoki, H. Miura, M. Ohtsuka, et al., PiggyBac transposon-mediated gene delivery efficiently generates stable transfectants derived from cultured primary human deciduous tooth dental pulp cells (HDDPCs) and HDDPC-derived iPS cells, Int. J. Oral Sci. 7 (3) (2015) 144–154.
[19] T. Schluep, J. Hwang, J. Cheng, J.D. Heidel, D.W. Bartlett, B. Hollister, et al., Preclinical efficacy of the camptothecin-polymer conjugate IT-101 in multiple cancer models, Clin. Canc. Res. 12 (5) (2006) 1606–1614.
[20] S.K. Huang, E. Mayhew, S. Gilani, D.D. Lasic, F.J. Martin, D. Papahadjopoulos, Pharmacokinetics and therapeutics of sterically stabilized liposomes in mice bearing C-26 colon carcinoma, Cancer Res. 52 (24) (1992) 6774–6781.
[21] D. Zhao, P. Chen, H. Yang, Y. Wu, X. Zeng, Y. Zhao, et al., Live attenuated measles virus vaccine induces apoptosis and promotes tumor regression in lung cancer, Oncol. Rep. 29 (1) (2013) 199–204.
[22] M. Loetscher, B. Gerber, P. Loetscher, S.A. Jones, L. Piali, I. Clark-Lewis, et al., Chemokine receptor specific for IP10 and mig: structure, function, and expression in activated T-lymphocytes, J. Exp. Med. 184 (3) (1996) 963–969.
[23] C. Sawyers, Targeted cancer therapy, Nature 432 (7015) (2004) 294.
[24] M. Mohammadi, M.R. Jaafari, H.R. Mirzaei, H. Mirzaei, Mesenchymal stem cell: a new horizon in cancer gene therapy, Canc. Gene Ther. 23 (9) (2016) 285–286.
[25] O.N. Koc, S.L. Gerson, B.W. Cooper, S.M. Dyhouse, S.E. Haynesworth, A.I. Caplan, et al., Rapid hematopoietic recovery after coinfusion of autologous-blood stem cells and culture-expanded marrow mesenchymal stem cells in advanced breast cancer patients receiving high-dose chemotherapy, J. Clin. Oncol. 18 (2) (2000) 307–316.
[26] P.A. Conget, J.J. Minguell, Adenoviral-mediated gene transfer into ex vivo expanded human bone marrow mesenchymal progenitor cells, Exp. Hematol. 28 (4) (2000) 382–390.
[27] H. Tsuda, T. Wada, Y. Ito, H. Uchida, H. Dehari, K. Nakamura, et al., Efficient BMP2 gene transfer and bone formation of mesenchymal stem cells by a fiber-mutant adenoviral vector, Mol. Ther. 7 (3) (2003) 354–365.
[28] K. Lee, M.K. Majumdar, D. Buyaner, J.K. Hendricks, M.F. Pittenger, J.D. Mosca, Human mesenchymal stem cells maintain transgene expression during expansion and differentiation, Mol. Ther. 3 (6) (2001) 857–866.
[29] O.N. Koc, J. Day, M. Nieder, S.L. Gerson, H.M. Lazarus, W. Krivit, Allogeneic mesenchymal stem cell infusion for treatment of metachromatic leukodystrophy (MLD) and Hurler syndrome (MPS-IH), Bone Marrow Transplant. 30 (4) (2002) 215–222.
[30] H.M. Lazarus, O.N. Koc, S.M. Devine, P. Curtin, R.T. Maziarz, H.K. Holland, et al., Cotransplantation of HLA-identical sibling culture-expanded mesenchymal stem cells and hematopoietic stem cells in hematologic malignancy patients, Biol. Blood Marrow Transplant. 11 (5) (2005) 389–398.
[31] J.M. Ryan, F.P. Barry, J.M. Murphy, B.P. Mahon, Mesenchymal stem cells avoid allogeneic rejection, J. Inflamm. 2 (2005) 8.
[32] H. Sahin, E. Borkham-Kamphorst, O.N. do, M.L. Berres, M. Kaldenbach, P. Schmitz, et al., Proapoptotic effects of the chemokine, CXCL 10 are mediated by the noncognate receptor TLR4 in hepatocytes, Hepatology 57 (2) (2013) 797–805.
[33] J.W. Marlin, Y.W. Chang, M. Ober, A. Handy, W. Xu, R. Jakobi, Functional PAK-2 knockout and replacement with a caspase cleavage-deficient mutant in mice reveals differential requirements of full-length PAK-2 and caspase-activated PAK-2p34, Mamm. Genome 22 (5–6) (2011) 306–317.
[34] C.C. Yates-Binder, M. Rodgers, J. Jaynes, A. Wells, R.J. Bodnar, T. Turner, An IP-10 (CXCL10)-derived peptide inhibits angiogenesis, PLoS One 7 (7) (2012) 16.
[35] M. Fujita, X. Zhu, R. Ueda, K. Sasaki, G. Kohanbash, E.R. Kastenhuber, et al., Effective immunotherapy against murine gliomas using type 1 polarizing dendritic cells–significant roles of CXCL10, Cancer Res. 69 (4) (2009) 1587–1595.
[36] X.L. Lu, X.B. Jiang, R.E. Liu, S.M. Zhang, The enhanced anti-angiogenic and antitumor effects of combining flk1-based DNA vaccine and IP-10, Vaccine 26 (42) (2008) 5352–5357.
[37] D.A. Arenberg, S.L. Kunkel, P.J. Polverini, S.B. Morris, M.D. Burdick, M.C. Glass, et al., Interferon-gamma-inducible protein 10 (IP-10) is an angiostatic factor that inhibits human non-small cell lung cancer (NSCLC) tumorigenesis and spontaneous metastases, J. Exp. Med. 184 (3) (1996) 981–992.
[38] C. Banissi, F. Ghiringhelli, L. Chen, A.F. Carpentier, Treg depletion with a low-dose metronomic temozolomide regimen in a rat glioma model, Cancer Immunol. Immunother. 58 (10) (2009) 1627–1634.
[39] M. Zabala, J.J. Lasarte, C. Perret, J. Sola, P. Berraondo, M. Alfaro, et al., Induction of immunosuppressive molecules and regulatory T cells counteracts the antitumor effect of interleukin-12-based gene therapy in a transgenic mouse model of liver cancer, J. Hepatol. 47 (6) (2007) 807–815.
[40] T.J. Curiel, G. Coukos, L. Zou, X. Alvarez, P. Cheng, P. Mottram, et al., Specific recruitment of regulatory T cells in ovarian carcinoma fosters immune privilege and predicts reduced survival, Nat. Med. 10 (9) (2004) 942–949.
[41] J. Fu, D. Xu, Z. Liu, M. Shi, P. Zhao, B. Fu, et al., Increased regulatory T cells correlate with CD8 T-cell impairment and poor survival in hepatocellular carcinoma patients, Gastroenterology 132 (7) (2007) 2328–2339.
[42] J. Ye, C. Ma, F. Wang, E.C. Hsueh, K. Toth, Y. Huang, et al., Specific recruitment of gammadelta regulatory T cells in human breast cancer, Cancer Res. 73 (20) (2013) 6137–6148.
[43] S. Lunardi, S.Y. Lim, R.J. Muschel, T.B. Brunner, IP-10/CXCL10 attracts regulatory T cells: implication for pancreatic cancer, OncoImmunology 4 (9) (2015).
[44] S. Lunardi, N.B. Jamieson, S.Y. Lim, K.L. Griffiths, M. Carvalho-Gaspar, O. Al-Assar, et al., IP-10/CXCL10 induction in human pancreatic cancer stroma influences lymphocytes recruitment and correlates with poor survival, Oncotarget 5 (22) (2014) 11064–11080.
[45] D. Datta, J.A. Flaxenburg, S. Laxmanan, C. Geehan, M. Grimm, A.M. Waaga-Gasser, et al., Ras-induced modulation of CXCL10 and its receptor splice variant CXCR3-B in MDA-MB-435 and MCF-7 cells: relevance for the development of human breast cancer, Cancer Res. 66 (19) (2006) 9509–9518.